

Visualizing the Propagation of Acute Lung Injury

Maurizio Cereda, M.D., Yi Xin, M.S., Natalie Meeder, B.A., Johnathan Zeng, B.S.E., YunQing Jiang, M.S.E., Hooman Hamedani, M.S., Harrilla Profka, D.V.M., Stephen Kadlecek, Ph.D., Justin Clapp, Ph.D., Charuhas G. Deshpande, M.D., Jue Wu, Ph.D., James C. Gee, Ph.D., Brian P. Kavanagh, M.B., Rahim R. Rizi, Ph.D.

ABSTRACT

Background: Mechanical ventilation worsens acute respiratory distress syndrome, but this secondary “ventilator-associated” injury is variable and difficult to predict. The authors aimed to visualize the propagation of such ventilator-induced injury, in the presence (and absence) of a primary underlying lung injury, and to determine the predictors of propagation.

Methods: Anesthetized rats ($n = 20$) received acid aspiration (hydrochloric acid) followed by ventilation with moderate tidal volume (V_T). In animals surviving ventilation for at least 2 h, propagation of injury was quantified by using serial computed tomography. Baseline lung status was assessed by oxygenation, lung weight, and lung strain (V_T /expiratory lung volume). Separate groups of rats without hydrochloric acid aspiration were ventilated with large ($n = 10$) or moderate ($n = 6$) V_T .

Results: In 15 rats surviving longer than 2 h, computed tomography opacities spread outward from the initial site of injury. Propagation was associated with higher baseline strain (propagation *vs.* no propagation [mean \pm SD]: 1.52 ± 0.13 *vs.* 1.16 ± 0.20 , $P < 0.01$) but similar oxygenation and lung weight. Propagation did not occur where baseline strain was less than 1.29. In healthy animals, large V_T caused injury that was propagated inward from the lung periphery; in the absence of preexisting injury, propagation did not occur where strain was less than 2.0.

Conclusions: Compared with healthy lungs, underlying injury causes propagation to occur at a lower strain threshold and it originates at the site of injury; this suggests that tissue around the primary lesion is more sensitive. Understanding how injury is propagated may ultimately facilitate a more individualized monitoring or management. (**ANESTHESIOLOGY 2016; 124:121-31**)

MECHANICAL ventilation at lower tidal volume (V_T) has been shown to improve survival in acute respiratory distress syndrome (ARDS),¹ suggesting that V_T reduction protects against ventilator-induced lung injury (VILI) by reducing inspiratory strain. To best limit damage, it might be important to detect early changes in vulnerable lung and to accurately determine the propensity for VILI. However, the onset of VILI is poorly characterized in the clinical setting, and it is almost always superimposed upon an underlying primary pulmonary lesion (*e.g.*, aspiration, pneumonia, or contusion).² Unfortunately, animal models with predictable (and short) courses of injury do not reproduce the variability observed in patients.

Computed tomography (CT) suggested that lung affected with ARDS is composed of an atelectatic (dependent) region and a normally aerated (nondependent) region.³ In this two-compartment model, the aerated “baby” lung preferentially receives the bulk of each V_T but comprises a significantly smaller available volume than the lungs in a healthy subject. Because inflammation predominates in this “aerated”

What We Already Know about This Topic

- Mechanical ventilation can damage uninjured lungs, but more commonly it worsens previously injured lungs (*e.g.*, aspiration or infection); however, secondary injury from mechanical ventilation is unpredictable and its propagation has never been visualized.

What This Article Tells Us That Is New

- Sequential computed tomography illustrates how lung strain, but not hypoxemia, predicts the spatial propagation of lung injury after acid aspiration. Lung regions near the initial injury focus may be more vulnerable to injury propagation by mechanical ventilation.

region,^{4,5} measuring strain and visualizing the propagation of lung injury in the aerated lung could predict and characterize the trajectory of VILI.

However, in many patients with ARDS, the aerated and nonaerated lung is not clearly delineated into two distinct compartments. Instead, the radiologic pattern may be of diffusely distributed moderately aerated tissue.⁶ Although the volume of aerated lung may be appreciable in diffuse injury,⁷

This article is featured in “This Month in Anesthesiology,” page 1A. Supplemental Digital Content is available for this article. Direct URL citations appear in the printed text and are available in both the HTML and PDF versions of this article. Links to the digital files are provided in the HTML text of this article on the Journal’s Web site (www.anesthesiology.org).

Submitted for publication April 23, 2015. Accepted for publication September 4, 2015. From the Departments of Anesthesiology and Critical Care (M.C., N.M.), Radiology (Y.X., J.Z., Y.J., H.H., H.P., S.K., J.C., J.W., J.C.G., R.R.R.), and Pathology and Laboratory Medicine (C.G.D.), University of Pennsylvania, Philadelphia, Pennsylvania; and Department of Anesthesia, Hospital for Sick Children, University of Toronto, Toronto, Ontario, Canada (B.P.K.).

Copyright © 2015, the American Society of Anesthesiologists, Inc. Wolters Kluwer Health, Inc. All Rights Reserved. Anesthesiology 2016; 124:121-31

aerated and nonaerated lungs are colocalized such that lung tissue interdependence^{8,9} may be important. It is unlikely that the same relation among inflation, deformation, and injury is at play when a given V_T inflates a separate aerated lung compartment compared with where aeration and nonaeration are diffusely intermingled. Heterogeneous tissue inflates in nonuniform manner, which can increase the strain in some microenvironments.¹⁰ In fact, recent CT findings indicate that variably aerated regions surrounding a primary locus of injury predict ARDS mortality.¹¹ Thus, the distribution of aerated lung in ARDS could be a factor in determining how injury is propagated during mechanical ventilation. If true, this could help identify the most beneficial approaches and adjuncts to ventilation (*e.g.*, very low V_T and prone positioning) that are appropriate in any given patient.

In the current study, we used sequential CT to investigate the relation between the spatial distribution of aerated/nonaerated lung and the tendency of injury to propagate during mechanical ventilation. In an *in vivo* rat model of acid aspiration with variable injury trajectory, we sought predictors of its propagation. We hypothesized that secondary VILI originates adjacent to the primary lesions—due to the local diffuse intermingling of aerated and collapsed tissues—and propagates concentrically and in proportion to strain. Such a pattern was contrasted with observations in lungs that were free of preexisting injury, where VILI has been shown to originate in the lung periphery,¹² and in the setting of the “baby lung” appears to become generalized across the normally aerated lung tissue.⁴

Materials and Methods

Male Sprague–Dawley rats were studied with approval by the Institutional Animal Care and Use Committee of the University of Pennsylvania (Philadelphia, Pennsylvania). The experimental protocol is described in full in Supplemental Digital Content 1, <http://links.lww.com/ALN/B205>. General anesthesia and paralysis were induced and maintained with intraperitoneal pentobarbital and IV pancuronium bromide; the trachea was intubated; and peak inspiratory pressure (PIP), dynamic compliance, heart rate, blood pressure, and arterial blood gases were measured. Rats were ventilated in the supine position with a small animal ventilator. All animals received intraperitoneal and IV hydration. After euthanasia, lungs were fixed, sliced in the coronal plane, stained, and reviewed by a pathologist (C.G.D.). Two groups of rats were studied.

Acid Aspiration with Moderate VT

We studied 20 ventilated rats (weighing 353 ± 26 g) after hydrochloric acid (HCl 2.5 ml/kg, pH 1.25) intratracheal. Because we aimed to investigate secondary progression of *mild* primary lung injury, no randomization was performed and animals were recruited sequentially. Only rats that survived long enough to display the propagation were studied. HCl was injected in two aliquots with the animal in the right and left lateral positions and 45° head elevation. Rats were

immediately returned to the supine position and allowed to stabilize while ventilated with positive end-expiratory pressure (PEEP) 10 cm H₂O and V_T 6 ml/kg for 1 h. In pilot experiments with this HCl dose, we confirmed heterogeneous distribution of HCl solution and variable course of injury in ventilated rats. After stabilization, ventilation continued for 3 h with moderate V_T (12 ml/kg, PEEP 3 cm H₂O, F_{IO_2} 1.0, and frequency 53 min⁻¹; fig. 1). Six additional healthy rats (weighing 365 ± 28 g) were ventilated for 3 h with these settings to show the radiological and physiological effects of moderate V_T ventilation in the absence of underlying lung injury.

Healthy Animals with Large VT

To compare the pattern of secondary propagation of pre-existing lung injury with the evolution of VILI in the absence of primary injury, we ventilated a separate group of 10 healthy rats (V_T 30 ml/kg, PEEP 0 cm H₂O, F_{IO_2} 0.5, and f 27 min⁻¹) for up to 3 h or until PIP increased by 50% (fig. 1). A broad range of body weights (360 to 600 g) was used to ensure variable lung volumes.

Computed Tomography

High-resolution whole-lung CT scans were acquired and reconstructed to three-dimensional whole-lung maps with 200- μ m isotropic resolution. Imaging was ventilator gated and performed during 500-ms breath holds. After acid aspiration, inspiratory and expiratory images were obtained at baseline and repeated hourly (fig. 1) without changing V_T . In healthy rats, imaging was repeated more often if PIP increased rapidly, and V_T was reduced to 12 ml/kg (f 53 min⁻¹) during CT acquisitions to facilitate comparisons with the other group.

Image Analysis

For each inspiratory image, three independent evaluators, blinded to group assignment, semiquantitatively¹³ rated (0 to 4) the spatial extension of high-density (ground

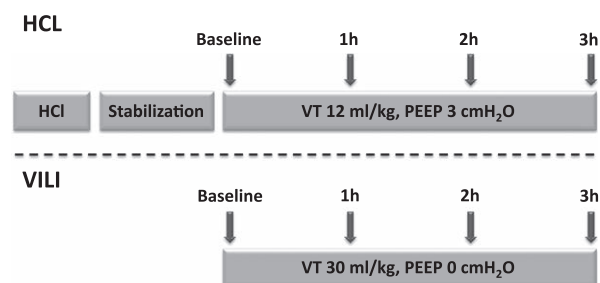


Fig. 1. Experimental timeline in rats ventilated with moderate tidal volume (V_T) after hydrochloric acid (HCl) aspiration (*top*) and in previously healthy rats with ventilator-induced lung injury (VILI) by large V_T ventilation (*bottom*). In rats with aspiration, imaging was performed without interrupting moderate V_T ventilation. In healthy rats, high-volume ventilation was suspended, and V_T was set at 12 ml/kg during each image acquisition, including baseline. PEEP = positive end-expiratory pressure.

glass and consolidations) tissue in four central and in four peripheral sectors of three coronal (frontal-to-dorsal) and three axial (apical-to-basal) slices. Observers set image contrast to a fixed intensity window (2,000 Hounsfield Unit) and level (-1,000). A global injury score was obtained at each time point; partial scores were also obtained in ventral and in dorsal areas. For quantitative CT analysis, three-dimensional whole-lung regions of interest were obtained by semiautomated, multilandmark, registration-based lung segmentation methodology (the delineation of lung borders from surrounding structures) developed by the authors.¹⁴ By using established methods¹⁵ of CT density analysis, each voxel was partitioned in air and tissue, allowing to quantify lung weight, end-inspiratory lung volume, and end-expiratory lung volume (EELV); lung strain was defined as $V_T/EELV$.^{16,17} The total weight of the lungs was partitioned among tissue compartments with different aeration (normo-aerated, poorly aerated, nonaerated, and hyperinflated tissue).¹⁸ Tidal recruitment (the weight of lung that collapses and reopens after each inspiration) was also calculated.¹⁸

Statistical Analysis

The sample size was decided based on pilot studies where we noticed a survival rate of approximately 75% at 2 h and of 50% at 3 h, which allowed us to study propagation and to test whether baseline characteristics (chosen *a priori*) were predictive of such propagation. For semiquantitative CT analysis, interobserver agreement was expressed using the quadratic weighted κ statistic, a test to compare two raters who use a categorically ordered measurement scale.¹⁹ Because there were three raters, κ was calculated three times for each rat between the three possible pairs of data. Correlations between variables were tested by linear regression. φ -Coefficient was calculated as a measure of association for binary variables. To study the relations between baseline variables and the propagation of injury in the lung, multiple ANOVA tests were performed separately for nonimaging and imaging markers followed by *post hoc t* tests to specifically identify which means were significantly different from each other. Bonferroni adjustment was performed for multiple *post hoc* comparisons. Repeated-measurements two-way ANOVA was conducted to examine the main effects of time on CT-derived and physiological variables. Binary variables were tested by using Fischer exact test. *P* value less than 0.05 (for two-tailed testing) was considered significant. Statistical analysis was performed by using "R" (R Foundation for Statistical Computing, Austria, available at: <http://www.R-project.org>) applications developed in the authors' laboratory.

Results

Underlying Injury Present

Of the 20 rats that received HCl, 5 were excluded from the analysis because of severe postaspiration hypoxemia ($P_{aO_2}/F_{iO_2} < 300$ mmHg; $n = 2$) or short survival less than 2 h

($n = 3$), precluding the quantification of injury propagation (baseline characteristics of this subgroup are shown in Supplemental Digital Content 2, <http://links.lww.com/ALN/B206>). In the 15 rats that survived longer than 2 h, baseline (*i.e.*, postaspiration) CT demonstrated circumscribed lesions in the dorsal lung (fig. 2). Two radiological patterns of injury were observed in this cohort: "diffuse" (propagated; fig. 2A) and contained (fig. 2B). The evolution of lung injury is also illustrated by animations accessible in Supplemental Digital Content 3, <http://links.lww.com/ALN/B207>, and Supplemental Digital Content 4, <http://links.lww.com/ALN/B208>. Both animations were obtained by combining sequential CT scans in the coronal slice in two animals after HCl aspiration. Propagation was centrifugal in both animals. Injury progression—reflected in the radiologic injury score (fig. 3A)—was accompanied by decreased EELV (fig. 3B) and increased lung weight (fig. 3C). Propagation of injury, defined by greater than 100% increase in score after 2 h of ventilation with moderate V_T , occurred in six animals (of which five died before 3 h).

Two approaches were taken to analyzing the HCl aspiration cohort. First, all 15 rats were considered as a single group. Second, animals were divided into two subgroups based on radiological injury propagation (*i.e.*, propagated *vs.* contained).

Whole-group Analysis

During the experiments, oxygenation, EELV, PIP, and compliance were all impaired, and estimated lung weight (edema) increased, consistent with progressive lung injury (table 1). The radiologic injury score increased from 37.6 ± 10.2 to 58.2 ± 22.8 to 101.8 ± 60.3 at baseline, 1 h, and end of the experiment, respectively ($F_{2,42} = 11.35$, $P < 0.001$); these increases in injury score were closely correlated with increases in individual lung weights ($R^2 = 0.75$, $P < 0.001$). The κ statistic for agreement among raters for the injury score was 0.91 ± 0.05 (three observers).

For comparison, healthy rats (no HCl) ventilated with identical settings had no radiological changes (at baseline and after 3 h) and minimal worsening in mechanics and gas exchange at 3 h (baseline and 3 h data for these rats are shown in the table in Supplemental Digital Content 5, <http://links.lww.com/ALN/B209>).

Propagation versus Containment: Subgroup Analysis

Five animals (five of six) died in the propagation subgroup *versus* none (zero of nine) in the containment subgroup ($\varphi = 0.87$, $P = 0.002$). Although the overall injury scores were similar in both groups at baseline, the injury was considerably increased (\approx four-fold) in the propagation group at 2 h and minimally increased in the containment group (table 2).

At baseline, gas exchange and hemodynamic variables (P_{aO_2} , P_{aCO_2} , lactate, and arterial blood pressure) were not significantly different between propagation and containment subgroups ($F_{1,13} = 1.44$, $P = 0.253$) (table 2). The two groups

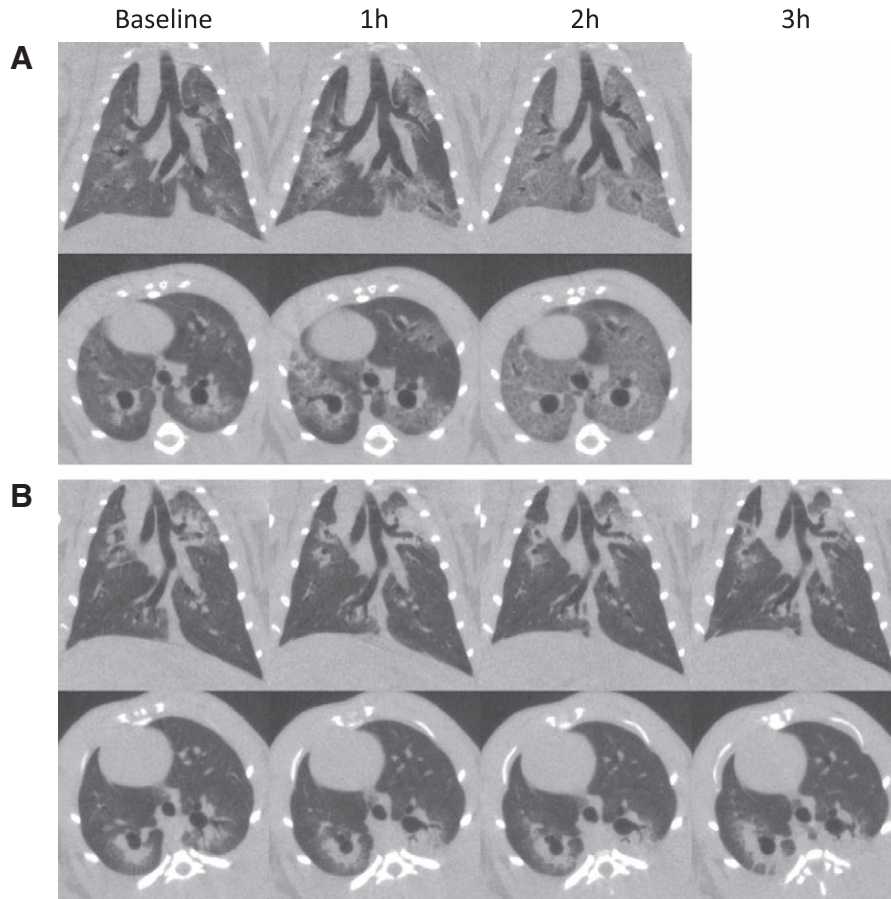


Fig. 2. Radiological injury propagation in two representative rats. Images were obtained after acid aspiration (after a period of stabilization of 1 h) and were repeated hourly. Coronal (A) and axial (B) images are shown. One animal (*top panel*) showed rapidly spreading radiological infiltrates and died after 2 h of ventilation. The second animal (*bottom panel*) had limited injury propagation and survived until the end of the experiment.

were significantly different ($F_{1,13} = 6.67$, $P = 0.023$) as judged by the baseline mechanical properties of the lung (strain, compliance, and EELV) (table 2). Further *post hoc* tests showed that, among these variables, lung strain was the major source of this significant difference (1.52 ± 0.13 vs. 1.16 ± 0.20 ; 31% difference; $F_{1,13} = 19.02$, $P_{Adj} = 0.002$), whereas the two groups did not show a significantly different compliance ($F_{1,13} = 6.46$, $P_{Adj} = 0.074$). Finally, EELV was significantly lower in the propagation cohort ($F_{1,13} = 9.80$, $P_{Adj} = 0.024$). At baseline, there was no overlap of the individual lung strain values between the two groups, but there was considerable overlap in P_{aO_2} and compliance (fig. 4, A–C). We found no differences in tidal recruitment and in the aeration partitioning (by tissue weight) between propagation and containment subgroups (see table, Supplemental Digital Content 6, <http://links.lww.com/ALN/B210>, which shows the results of the quantitative analysis of CT density distributions).

During ventilation with moderate V_T , the decreases in P_{aO_2} , EELV, and compliance were greater in the propagation versus containment groups. Although the estimated lung weight increased by 30% in the propagation group, it was unchanged in the containment group (table 2).

Injury scores at baseline were higher in the dorsal versus ventral regions in both groups (no between-group differences); during ventilation, the injury spread to the ventral regions in the propagation group, but not in the containment group (table 2).

Histological analysis in four rats (two in propagation and two in containment groups) confirmed inflammatory injury, displaying edema, intraalveolar and perivascular neutrophils, and hyaline membranes (fig. 5). These changes were ubiquitous in animals with radiological propagation, but they were spatially more limited in contained injury. By the end of the experiment, the topographic distribution of the histologic injury corresponded to the radiological injury scoring (fig. 5).

Relation between Lung Strain and Injury Propagation

To further examine the correlation between strain and injury propagation, we plotted the increase of injury score in the first hour of ventilation versus baseline strain. This plot and regression line ($P = 0.01$) are shown in the figure in Supplemental Digital Content 7, <http://links.lww.com/ALN/B211>, and suggest minimal propagation at lower strain. Therefore, we divided the overall population of the HCl cohort into

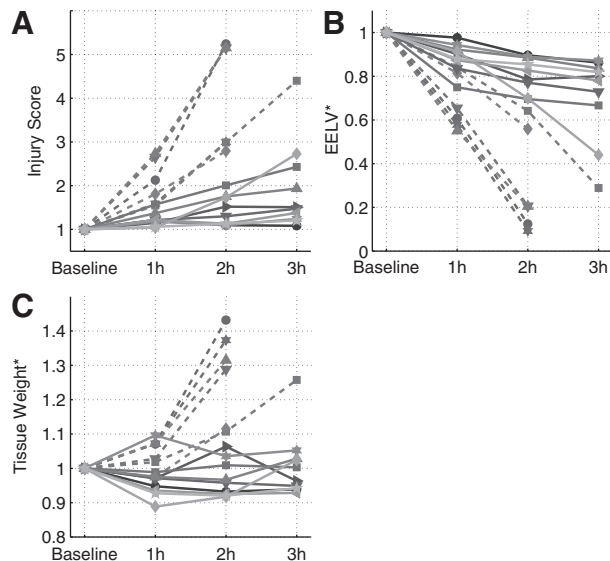


Fig. 3. Individual trends of (A) radiological injury score, (B) end-expiratory lung volume (EELV), and (C) estimated lung weight after acid aspiration. All variables were measured by computed tomography during ventilation and are expressed as fraction of the baseline values obtained after acid aspiration. *Dashed lines* represent animals with radiological propagation of lung injury (score more than doubled within the first 2 h).

two subgroups with baseline strain greater than or less than or equal to the median value (1.3). In animals with baseline strain above the median, mortality was higher and propagation was more marked; in addition, injury scores and gain in lung weight were greater (table 3).

Underlying Injury Absent, Large V_T

Ventilation with large V_T caused injury in all animals within 3 h and death before 2 h in five animals. Injury started in the lung periphery and rapidly progressed toward the lung hilum (fig. 6A). The animation illustrating the evolving injury is shown in Supplemental Digital Content 8, <http://links.lww.com/ALN/B212>. Lung weight increased from 3.7 ± 0.4 to 6.9 ± 1.3 g ($P < 0.00001$), EELV decreased from 3.5 ± 0.9 to 1.2 ± 1.1 ml ($P < 0.0001$), the lung injury score reached 162.5 ± 37.1 , and histological abnormalities were widespread

(fig. 6B). The baseline strain (4.2 ± 0.8 ; range 3.0 to 5.3) was markedly higher than in the rats with acid aspiration (table 2) and was correlated with the hourly increase of injury score ($R^2 = 0.73$, $P < 0.002$; fig. 7).

Discussion

To the best of our knowledge, the current study provides the first reported visualization of the propagation of lung injury (see animations in Supplemental Digital Content 3, <http://links.lww.com/ALN/B207>, Supplemental Digital Content 4, <http://links.lww.com/ALN/B208>, and Supplemental Digital Content 8, <http://links.lww.com/ALN/B212>). Our key finding is the nature of VILI propagation in the presence or absence of an underlying (primary) lesion. When VILI complicated a preexisting lesion, it started at that lesion and was propagated concentrically toward the rest of the lung. By contrast, when VILI was induced as the primary injury in previously healthy lungs, it originated in peripheral lung regions and spread centrally toward the hilum. Furthermore, we found that although impaired oxygenation was not a predictor of injury propagation in preinjured animals, strain predicted propagation in both cohorts. These findings suggest that it may ultimately be possible to predict (and perhaps prevent) propagation of injury and thereby minimize its generalization.

Our data on VILI progression in previously healthy lungs agree with the small body of previous work, including ours,²⁰ on this topic.^{12,21–23} When VILI was induced as the primary injury, it originated in peripheral regions and rapidly disseminated centrally toward the hilum. Primary VILI was proportional to strain, also corroborating previous research.¹⁶ Dorsobasilar localization of unstable atelectasis²¹ and strain²⁴ can partly explain this VILI distribution. In healthy supine rats, we found that dependent airspaces undergo larger dimensional changes during recruitment–derecruitment.²⁵ In contrast, when VILI complicated a preexisting lesion, it started at the underlying lesion and propagated concentrically to the rest of the lung; this secondary VILI was also strain dependent. Although VILI cannot be directly differentiated from aspiration, the worsening of preexisting injury was less likely caused by direct extension of the initial

Table 1. Physiological Parameters Measured at Baseline and at the End of a Period of Moderate Tidal Volume Ventilation (12 ml/kg) after Acid Aspiration in Rats (n = 15)

	Baseline	End	P Value
Pao ₂ (mmHg)	439.3 ± 64.0	184.0 ± 169.4	0.00009
Paco ₂ (mmHg)	44.8 ± 7.7	51.0 ± 8.2	0.04
pH	7.336 ± 0.047	7.285 ± 0.072	0.02
Lactic acid (mEq/l)	1.4 ± 0.7	2.2 ± 1.3	0.07
ABP (mmHg)	116.9 ± 16.9	82.3 ± 32.0	0.003
PIP (cm H ₂ O)	22.1 ± 3.5	28.8 ± 5.2	0.000003
Compliance (ml/cm H ₂ O)	0.24 ± 0.04	0.18 ± 0.04	0.000005
EELV (ml)	3.56 ± 0.81	2.05 ± 1.23	0.000008
Lung weight (g)	4.30 ± 0.45	4.88 ± 1.11	0.04

ABP = arterial blood pressure; EELV = end-expiratory lung volume; PIP = peak inspiratory pressure.

Table 2. Markers of Lung Injury at Baseline (after Acid Aspiration) and after 2 h of Moderate Tidal Volume Ventilation

	Propagation (n = 6)		Containment (n = 9)	
	Baseline	2 h	Baseline	2 h
Body weight (g)	361 ± 26	—	349 ± 26	—
Pao ₂ (mmHg)	421.5 ± 72.1	80.2 ± 25.1*	451.2 ± 59.4	278.5 ± 158.3†
Lung weight (g)	4.29 ± 0.21	5.73 ± 1.09‡	4.30 ± 0.59	4.36 ± 1.04‡
Compliance (ml/cm H ₂ O)	0.21 ± 0.03	0.14 ± 0.02*	0.25 ± 0.03	0.21 ± 0.03*,‡
EELV (ml)	2.92 ± 0.30	0.90 ± 0.73*	3.99 ± 0.78§	3.20 ± 0.44*,‡
Lung strain	1.52 ± 0.13	—	1.16 ± 0.20‡	—
Injury score	39.3 ± 12.0	154.8 ± 45.1*	36.5 ± 9.4	51.0 ± 16.0*‡
Dorsal/ventral score	3.6 ± 0.8	1.4 ± 0.6*	4.8 ± 4.1	3.6 ± 3.2

Rats with propagation of lung injury were analyzed separately from those with more contained injury. Vertical distribution of lung injury was quantified by dividing partial scores measured in central over peripheral areas of interest. * $P < 0.01$ and † $P < 0.05$ vs. baseline; ‡ $P < 0.01$ and § $P < 0.05$ between groups. EELV = end-expiratory lung volume.

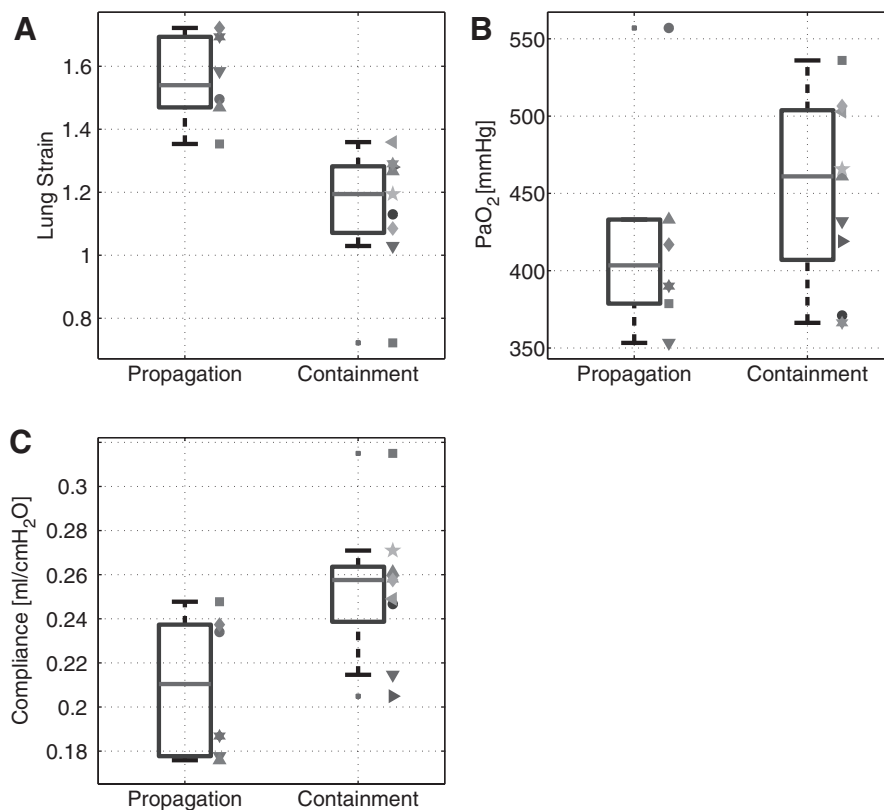


Fig. 4. Individual baseline values and summary statistics (median, interquartile range, and extremes of the distribution) of (A) lung strain, (B) compliance, and (C) PaO₂ in rats that had progression *versus* containment of lung injury while receiving moderate volume ventilation after acid aspiration. Individual subjects are indicated with symbols and colors matching those in figure 3.

insult. Rather, as predicted by the “baby lung” construct,³ it was more likely a consequence of subsequent ventilation at the indicated volumes. This interpretation is supported by studies comparing the effects of higher *versus* lower V_T in this model,²⁶ which showed that moderate V_T worsened the severity of injury after acid aspiration.

However, the baby lung model does not fully account for our observations here. Crucially, it cannot explain why secondary VILI spread locally outward from preinjured tissue. According to the baby lung theory, the “healthy” aerated

parenchyma in the injured rats should have been smaller than that in healthy animals but otherwise possessive of normal mechanical and biological characteristics; consequently, it should have displayed a centripetal propagation pattern suggestive of primary VILI. However, lung tissue at lesion margins had faster worsening of injury than at the lung periphery. It is consequently evident that injured lung makes proximal tissue more sensitive to strain.

We suggest that the vulnerability of this perilesional tissue can best be explained by local discontinuities of aeration.

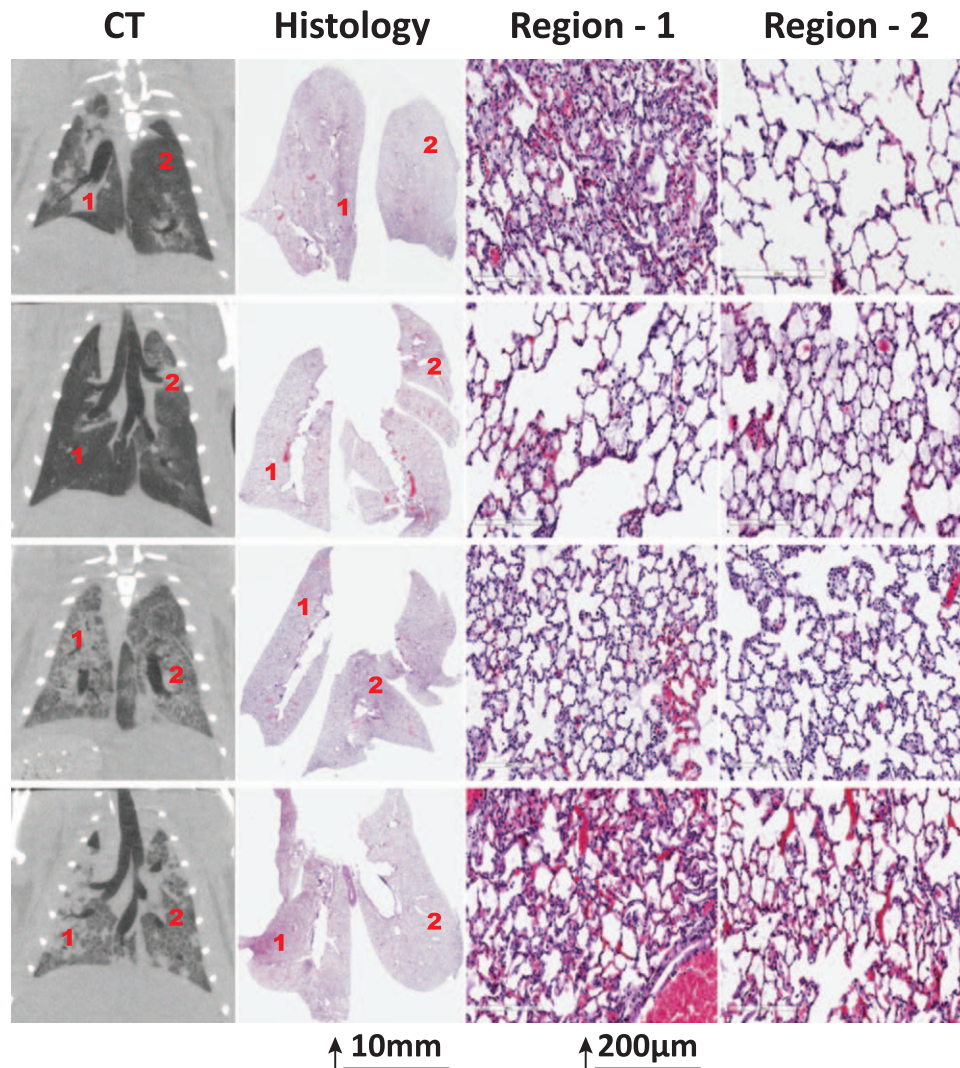


Fig. 5. Computed tomography (CT) and histological appearance of rat lungs with acid aspiration after ventilation with moderate tidal volume. Changes compatible with inflammatory injury were more widely disseminated in animals with larger extension of CT abnormalities.

Table 3. Evolution of Lung Injury in the First 2 h of Moderate Tidal Volume Ventilation in Rats with Higher vs. Lower Baseline Strain (> or ≤ Median) at Baseline after Acid Aspiration

	Baseline Strain > 1.29	Baseline Strain ≤ 1.29	<i>P</i> Value
Injury propagation/total	6/7	0/8	0.0014
Death/total	5/7	0/8	0.007
Change of injury score	99.8 ± 55.9	15.6 ± 12.0	0.001
Change of lung weight (g)	1.19 ± 1.22	-0.12 ± 0.24	0.01

Regions of intermediate CT attenuation (between -100 and -500 HU) concentric to the injury core were consistently visible in the initial CT scans (see Supplemental Digital Content 9, <http://links.lww.com/ALN/B213>, which shows binary maps of lung aeration). This radiological pattern indicates decreased but not absent gas content, compatible with subvoxel codispersion of well-ventilated and nonventilated

airspace. Functional CT studies have shown hyperventilation within poorly aerated lung regions,⁷ perhaps caused by reciprocal dilation of ventilated airspaces near collapsed (*i.e.*, microatelectasis)⁸ or fluid-filled alveoli²⁷; similarly, using hyperpolarized diffusion magnetic resonance imaging, we observed inspiratory dilatation of residual ventilated airspaces in poorly recruited lungs.²⁸ Moderate strain may worsen injury beginning near initial lesions (*cf.*, fig. 2) because tissue with discontinuous aeration is more exposed to local augmentation of inspiratory stress.¹⁰ Recent clinical findings have lent credence to this hypothesis by demonstrating that the presence of small-scale heterogeneity of CT density predicts ARDS mortality.¹¹

It is important to note, however, that other mechanisms may contribute to local injury propagation near a primary injury. For example, systemic inflammation could sensitize pulmonary cells to mechanical stress.²⁹ But it is likely that circulating inflammatory mediators facilitate VILI globally

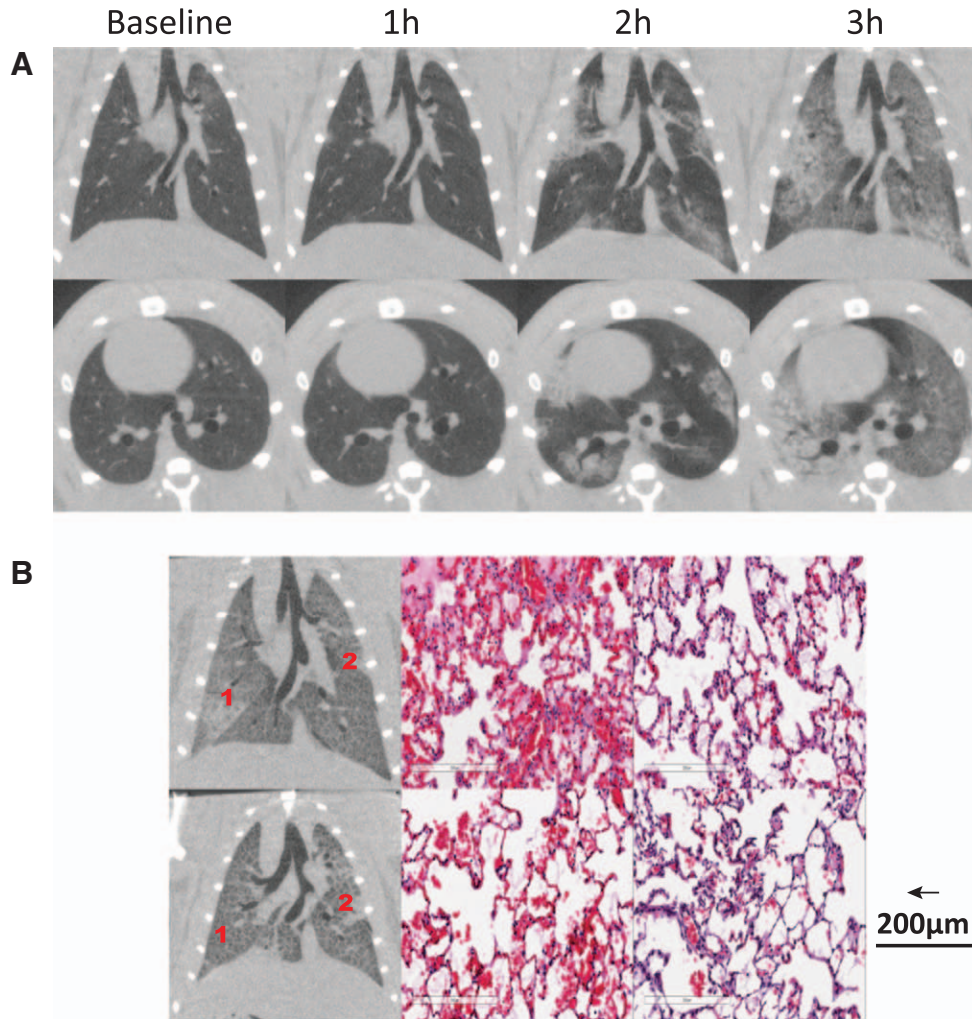


Fig. 6. (A) Radiological propagation of lung injury in healthy rats ventilated with high-stretch ventilation. Injury consistently started in the lung periphery and propagated toward the hilum. (B) Histological and radiological distribution of lesions in two rats of this group.

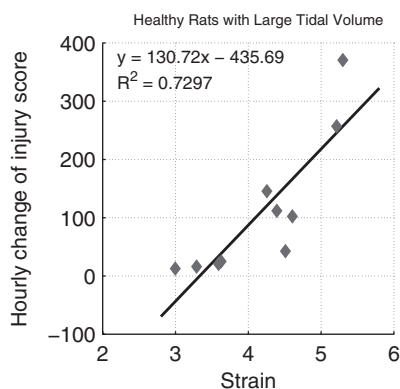


Fig. 7. Relation between the rate of propagation of ventilator-induced lung injury, expressed as the hourly increase in semi-quantitative radiological score, and the pulmonary strain at baseline during ventilation with tidal volume 30 ml/kg in previously healthy rats.

rather than locally because septic rats have faster VILI onset but identical dissemination compared with nonseptic animals.²⁰ In addition, endothelial gap junction communication

has been implicated in the propagation of lung edema and inflammation³⁰ after focal lesions by HCl. Furthermore, regional hyperperfusion³¹ could promote capillary stress failure and edema during ventilation.³² Finally, dissemination of airway fluid facilitated by mechanical ventilation³³ can spread injury in the distal airways.

The results of this study have two potential implications for the eventual management of patients with early lung injury. First, studying the spatial propagation of lung injury might facilitate the investigation of containment strategies. In contrast, studying established ARDS clouds understanding about the condition's initial evolution. Moreover, clinical definitions³⁴ omit the evolving distribution of injury, which may be especially important in ARDS that presents with nondiffuse injury.⁶

Second, our work is consistent with other studies emphasizing that protecting injured lungs from excessive strain is essential to mitigating ARDS.²⁶ To reduce strain, clinicians prescribe V_T according to a patient's predicted body weight.¹ However, recent studies have highlighted that

severely ill patients have smaller lung capacities³⁵ and are at risk of VILI even with smaller V_T .³⁶ Global lung strain can be measured at bedside with nonradiological instruments¹⁷ although regional stress distribution is missed.¹¹ Our work extends the relevance of strain to less severe injury, where lung capacity is preserved. This may be relevant in low V_T ventilation in patients without established ARDS³⁷ although we note that generalized use of low V_T can have undesired consequences such as atelectasis³⁸ and patient discomfort.³⁹ Although some data suggest no increase in sedation doses during low V_T ventilation,⁴⁰ this may change with the wider use of restricted sedation.⁴¹

Risk of propagation after HCl aspiration was not related to oxygenation. This suggests that baseline PaO_2/FiO_2 measurement has only a limited ability to characterize early lung injury and to predict its evolution. The hypoxemia that reflects severity in ARDS³⁴ is perhaps the end-result of complex maldistributions of ventilation and blood flow rather than a marker of injury progression. Within this context, pulmonary strain may be a more pertinent measurement for characterizing individual risk of ARDS progression.

Our study has important limitations. The design is not randomized because we aimed to study only animals (with limited injury) that were able to display propagation and to identify baseline predictors of such behavior. The exclusion of five rats with worse injury had probably minimal effects on our conclusions because their baseline mechanics (shown in Supplemental Digital Content 2, <http://links.lww.com/ALN/B206>) were also worse than in the main group. Because this was a short-term small-animal experiment, the data are difficult to extrapolate to a clinical context. For example, highly compliant chest wall in rats may attenuate the binary dorsal/ventral distribution of gas and atelectasis; however, baseline HCl injury was more represented dorsally. The serial CT imaging provides topographical descriptors of regional edema and atelectasis although histology corroborates the observed injury differences between propagated *versus* contained responses to high V_T (fig. 5). Because we used a semi-quantitative metric and a fixed grayscale to quantify injury propagation, subtle intersubject variability in aeration (*e.g.*, due to uneven acid delivery) could be underdetected. However, quantitative analysis (shown in Supplemental Digital Content 6, <http://links.lww.com/ALN/B210>) did not show differences between subgroups in lung density distribution. Methodology to measure strain is always complex, and overall lung deformation may not directly reflect the alveolar micro-environment.²⁵ Correctly relating injury propagation to VILI necessitated a pragmatic approach, and we chose to measure strain as the ratio between V_T and EELV¹⁷ rather than index V_T to functional residual capacity.⁴² This approach has been successfully used in patients with ARDS^{4,17} but yields lower strain values where PEEP (and thus, EELV) are increased. Thus, comparisons with animals in which PEEP was not used may result in bias. However, the low levels of PEEP were just sufficient to match EELV in injury *versus* control

groups at baseline (3.6 ± 0.9 ml after HCl *vs.* 3.5 ± 0.7 ml in healthy rats). We did not correct strain for tidal recruitment⁴² because this variable was not different between the propagation *versus* containment subgroups (see table, Supplemental Digital Content 6, <http://links.lww.com/ALN/B210>, with the results of quantitative CT density analysis). All rats were ventilated with high FiO_2 to optimize survival, but this (*vs.* ambient levels of FiO_2) may potentiate VILI⁴³; however, the responses of VILI to V_T and strain were similar to previously reported sham-operated animals ventilated with FiO_2 1.0.²⁰

Conclusions

We provide visual evidence of the spatial propagation of VILI. In the presence of preexisting injury, propagation begins in regions of primary injury and spreads concentrically; this is in contrast to the centripetal pattern of propagation—toward the hilum—observed in previously healthy lungs. In both cases, propagation is predicted by strain. Injury propagation in perilesional tissue may reflect the maldistribution of local lung inflation, which makes tissue more vulnerable to strain. Better knowledge of the process by which primary injury disseminates during ventilation could help quantify the risk of ARDS progression and thereby potentially optimize individual management.

Acknowledgments

This work was supported by the National Institutes of Health (Bethesda, Maryland) grant nos. R01-HL116342 and R01-HL124986. Dr. Cereda is supported by a grant from the Foundation for Anesthesia Education and Research (Schaumburg, Illinois), from the Society of Critical Care Anesthesiologists (Park Ridge, Illinois), and by the Transdisciplinary Awards Program in Translational Medicine and Therapeutics (Philadelphia, Pennsylvania). Dr. Kavanagh is supported by operating funds from the Canadian Institutes of Health Research (Ottawa, Ontario, Canada) and holds the Dr. Geoffrey Barker Chair in Critical Care Medicine (Hospital for Sick Children, University of Toronto, Toronto, Ontario, Canada).

Competing Interests

The authors declare no competing interests.

Correspondence

Address correspondence to Dr. Cereda: Department of Anesthesiology and Critical Care, Perelman School of Medicine, University of Pennsylvania, Dulles 773, 3400 Spruce Street, Philadelphia, Pennsylvania 19104. maurizio.cereda@uphs.upenn.edu. Information on purchasing reprints may be found at www.anesthesiology.org or on the masthead page at the beginning of this issue. ANESTHESIOLOGY's articles are made freely accessible to all readers, for personal use only, 6 months from the cover date of the issue.

References

1. Ventilation with lower tidal volumes as compared with traditional tidal volumes for acute lung injury and the acute respiratory distress syndrome. The Acute Respiratory Distress Syndrome Network. *N Engl J Med* 2000; 342:1301–8

2. Frank JA, Parsons PE, Matthay MA: Pathogenetic significance of biological markers of ventilator-associated lung injury in experimental and clinical studies. *Chest* 2006; 130:1906–14
3. Gattinoni L, Pesenti A, Avalli L, Rossi F, Bombino M: Pressure-volume curve of total respiratory system in acute respiratory failure. Computed tomographic scan study. *Am Rev Respir Dis* 1987; 136:730–6
4. Bellani G, Guerra L, Musch G, Zanella A, Patroniti N, Mauri T, Messa C, Pesenti A: Lung regional metabolic activity and gas volume changes induced by tidal ventilation in patients with acute lung injury. *Am J Respir Crit Care Med* 2011; 183:1193–9
5. Tsuchida S, Engelberts D, Peltekova V, Hopkins N, Frndova H, Babyn P, McKlerie C, Post M, McLoughlin P, Kavanagh BP: Atelectasis causes alveolar injury in nonatelectatic lung regions. *Am J Respir Crit Care Med* 2006; 174:279–89
6. Malbouisson LM, Muller JC, Constantin JM, Lu Q, Puybasset L, Rouby JJ; CT Scan ARDS Study Group: Computed tomography assessment of positive end-expiratory pressure-induced alveolar recruitment in patients with acute respiratory distress syndrome. *Am J Respir Crit Care Med* 2001; 163:1444–50
7. Bayat S, Porra L, Albu G, Suhonen H, Strengell S, Suortti P, Sovijärvi A, Peták F, Habre W: Effect of positive end-expiratory pressure on regional ventilation distribution during mechanical ventilation after surfactant depletion. *ANESTHESIOLOGY* 2013; 119:89–100
8. Mead J, Takishima T, Leith D: Stress distribution in lungs: A model of pulmonary elasticity. *J Appl Physiol* 1970; 28:596–608
9. Bachofen H, Gehr P, Weibel ER: Alterations of mechanical properties and morphology in excised rabbit lungs rinsed with a detergent. *J Appl Physiol Respir Environ Exerc Physiol* 1979; 47:1002–10
10. Mertens M, Tabuchi A, Meissner S, Krueger A, Schirrmann K, Kertzschner U, Pries AR, Slutsky AS, Koch E, Kuebler WM: Alveolar dynamics in acute lung injury: Heterogeneous distension rather than cyclic opening and collapse. *Crit Care Med* 2009; 37:2604–11
11. Cressoni M, Cadringer P, Chiurazzi C, Amini M, Gallazzi E, Marino A, Brioni M, Carlesso E, Chiumello D, Quintel M, Bugeo G, Gattinoni L: Lung inhomogeneity in patients with acute respiratory distress syndrome. *Am J Respir Crit Care Med* 2014; 189:149–58
12. Broccard A, Shapiro RS, Schmitz LL, Adams AB, Nahum A, Marini JJ: Prone positioning attenuates and redistributes ventilator-induced lung injury in dogs. *Crit Care Med* 2000; 28:295–303
13. Burnham EL, Hyzy RC, Paine R III, Coley C II, Kelly AM, Quint LE, Lynch D, Janssen WJ, Moss M, Standiford TJ: Chest CT features are associated with poorer quality of life in acute lung injury survivors. *Crit Care Med* 2013; 41:445–56
14. Xin Y, Song G, Cereda M, Kadlecsek S, Hamedani H, Jiang Y, Rajaei J, Clapp J, Profka H, Meeder N, Wu J, Tustison NJ, Gee JC, Rizi RR: Semiautomatic segmentation of longitudinal computed tomography images in a rat model of lung injury by surfactant depletion. *J Appl Physiol* (1985) 2015; 118:377–85
15. Denison DM, Morgan MD, Millar AB: Estimation of regional gas and tissue volumes of the lung in supine man using computed tomography. *Thorax* 1986; 41:620–8
16. Protti A, Cressoni M, Santini A, Langer T, Mietto C, Febres D, Chierichetti M, Coppola S, Conte G, Gatti S, Leopardi O, Masson S, Lombardi L, Lazzarini M, Rampoldi E, Cadringer P, Gattinoni L: Lung stress and strain during mechanical ventilation: Any safe threshold? *Am J Respir Crit Care Med* 2011; 183:1354–62
17. González-López A, García-Prieto E, Batalla-Solís E, Amador-Rodríguez L, Avello N, Blanch L, Albaiceta GM: Lung strain and biological response in mechanically ventilated patients. *Intensive Care Med* 2012; 38:240–7
18. Gattinoni L, Caironi P, Cressoni M, Chiumello D, Ranieri VM, Quintel M, Russo S, Patroniti N, Cornejo R, Bugeo G: Lung recruitment in patients with the acute respiratory distress syndrome. *N Engl J Med* 2006; 354:1775–86
19. Ludbrook J: Statistical techniques for comparing measurers and methods of measurement: A critical review. *Clin Exp Pharmacol Physiol* 2002; 29:527–36
20. Yehya N, Xin Y, Oquendo Y, Cereda M, Rizi RR, Margulies SS: Cecal ligation and puncture accelerates development of ventilator-induced lung injury. *Am J Physiol Lung Cell Mol Physiol* 2015; 308:L443–51
21. Sinclair SE, Chi E, Lin HI, Altmeier WA: Positive end-expiratory pressure alters the severity and spatial heterogeneity of ventilator-induced lung injury: An argument for cyclical airway collapse. *J Crit Care* 2009; 24:206–11
22. Nishimura M, Honda O, Tomiyama N, Johkoh T, Kagawa K, Nishida T: Body position does not influence the location of ventilator-induced lung injury. *Intensive Care Med* 2000; 26:1664–9
23. Cressoni M, Chiurazzi C, Gotti M, Amini M, Brioni M, Algieri I, Cammaroto A, Rovati C, Massari D, di Castiglione CB, Nikolla K, Montaruli C, Lazzarini M, Dondossola D, Colombo A, Gatti S, Valerio V, Gagliano N, Carlesso E, Gattinoni L: Lung inhomogeneities and time course of ventilator-induced mechanical injuries. *ANESTHESIOLOGY* 2015; 123:618–27
24. Hubmayr RD, Walters BJ, Chevalier PA, Rodarte JR, Olson LE: Topographical distribution of regional lung volume in anesthetized dogs. *J Appl Physiol Respir Environ Exerc Physiol* 1983; 54:1048–56
25. Cereda M, Xin Y, Emami K, Huang J, Rajaei J, Profka H, Han B, Mongkolwisetwara P, Kadlecsek S, Kuzma NN, Pickup S, Kavanagh BP, Deutschman CS, Rizi RR: Positive end-expiratory pressure increments during anesthesia in normal lung result in hysteresis and greater numbers of smaller aerated airspaces. *ANESTHESIOLOGY* 2013; 119:1402–9
26. Frank JA, Gutierrez JA, Jones KD, Allen L, Dobbs L, Matthay MA: Low tidal volume reduces epithelial and endothelial injury in acid-injured rat lungs. *Am J Respir Crit Care Med* 2002; 165:242–9
27. Perlman CE, Lederer DJ, Bhattacharya J: Micromechanics of alveolar edema. *Am J Respir Cell Mol Biol* 2011; 44:34–9
28. Cereda M, Emami K, Xin Y, Kadlecsek S, Kuzma NN, Mongkolwisetwara P, Profka H, Pickup S, Ishii M, Kavanagh BP, Deutschman CS, Rizi RR: Imaging the interaction of atelectasis and overdistension in surfactant-depleted lungs. *Crit Care Med* 2013; 41:527–35
29. Levine GK, Deutschman CS, Helfaer MA, Margulies SS: Sepsis-induced lung injury in rats increases alveolar epithelial vulnerability to stretch. *Crit Care Med* 2006; 34:1746–51
30. Parthasarathi K, Bhattacharya J: Localized acid instillation by a wedged-catheter method reveals a role for vascular gap junctions in spatial expansion of acid injury. *Anat Rec (Hoboken)* 2011; 294:1585–91
31. Richter T, Bergmann R, Knels L, Hofheinz F, Kasper M, Deile M, Pietzsch J, Ragaller M, Koch T: Pulmonary blood flow increases in damaged regions directly after acid aspiration in rats. *ANESTHESIOLOGY* 2013; 119:890–900
32. Broccard AF, Hotchkiss JR, Kuwayama N, Olson DA, Jamal S, Wangenstein DO, Marini JJ: Consequences of vascular flow on lung injury induced by mechanical ventilation. *Am J Respir Crit Care Med* 1998; 157(6 Pt 1):1935–42
33. de Prost N, Roux D, Dreyfuss D, Ricard JD, Le Guludec D, Saumon G: Alveolar edema dispersion and alveolar protein permeability during high volume ventilation: Effect of positive end-expiratory pressure. *Intensive Care Med* 2007; 33:711–7
34. Ranieri VM, Rubenfeld GD, Thompson BT, Ferguson ND, Caldwell E, Fan E, Camporota L, Slutsky AS; ARDS Definition

- Task Force: Acute respiratory distress syndrome: The Berlin Definition. *JAMA* 2012; 307:2526–33
35. Mattingley JS, Holets SR, Oeckler RA, Stroetz RW, Buck CF, Hubmayr RD: Sizing the lung of mechanically ventilated patients. *Crit Care* 2011; 15:R60
 36. Terragni PP, Rosboch G, Tealdi A, Corno E, Menaldo E, Davini O, Gandini G, Herrmann P, Mascia L, Quintel M, Slutsky AS, Gattinoni L, Ranieri VM: Tidal hyperinflation during low tidal volume ventilation in acute respiratory distress syndrome. *Am J Respir Crit Care Med* 2007; 175:160–6
 37. Serpa Neto A, Cardoso SO, Manetta JA, Pereira VG, Espósito DC, Pasqualucci Mde O, Damasceno MC, Schultz MJ: Association between use of lung-protective ventilation with lower tidal volumes and clinical outcomes among patients without acute respiratory distress syndrome: A meta-analysis. *JAMA* 2012; 308:1651–9
 38. Richard JC, Maggiore SM, Jonson B, Mancebo J, Lemaire F, Brochard L: Influence of tidal volume on alveolar recruitment. Respective role of PEEP and a recruitment maneuver. *Am J Respir Crit Care Med* 2001; 163:1609–13
 39. Kallet RH, Luce JM: Detection of patient-ventilator asynchrony during low tidal volume ventilation, using ventilator waveform graphics. *Respir Care* 2002; 47:183–5
 40. Kahn JM, Andersson L, Karir V, Polissar NL, Neff MJ, Rubenfeld GD: Low tidal volume ventilation does not increase sedation use in patients with acute lung injury. *Crit Care Med* 2005; 33:766–71
 41. Shehabi Y, Bellomo R, Reade MC, Bailey M, Bass F, Howe B, McArthur C, Seppelt IM, Webb S, Weisbrodt L; Sedation Practice in Intensive Care Evaluation (SPICE) Study Investigators; ANZICS Clinical Trials Group: Early intensive care sedation predicts long-term mortality in ventilated critically ill patients. *Am J Respir Crit Care Med* 2012; 186:724–31
 42. Chiumello D, Carlesso E, Cadringer P, Caironi P, Valenza F, Polli F, Tallarini F, Cozzi P, Cressoni M, Colombo A, Marini JJ, Gattinoni L: Lung stress and strain during mechanical ventilation for acute respiratory distress syndrome. *Am J Respir Crit Care Med* 2008; 178:346–55
 43. Sinclair SE, Altemeier WA, Matute-Bello G, Chi EY: Augmented lung injury due to interaction between hyperoxia and mechanical ventilation. *Crit Care Med* 2004; 32:2496–501